

Downward Continuation of Gongola Basin Residual Gravity Anomalies Using Density Log

E. E. Epuh¹, P. C. Nwilo¹, D. O. Olorode² and C. U. Ezeigbo¹

Abstract

The major ambiguity in the determination of the subsurface structures by the use of downward continuation is due to the existence of multiple interfaces. This is because residual gravity anomalies are the superposition of effects originating from several interfaces from the subsurface at once. The integration of density log helps in the delineation of the multiple interfaces using a weighting density function. Following pre-existing mathematical models, a new formulation for the weighting density function with respect to the wave numbers attenuation, depth and station intervals were established using the concept of equivalent stratum. The logs were stripped into shorter sections at constant intervals so as to generate a density contrast with respect to depth. This is meant to define the various interfaces, the upper and lower depth limits and the nature of the anomalous mass. From the results obtained, it was observed that the projected residual gravity anomalies showed some increase in amplitude with increase in depth. The weighted density function provided a good estimate of the maximum gravity

¹ Department of Surveying and Geoinformatics, University of Lagos,
e-mail: eeepuh@yahoo.com

² Physics Department, University of Lagos

effect that can be expected from a topographic feature of a given size which lies at a given depth and the fluctuation in the residual gravity anomaly values between negative and positive at intermediate levels showed that the attenuation was minimized. The upper and lower depth limits of the anomalous mass were defined as 2015m and 2170m and the density contrast between the upper and lower depth limits suggest that the anomalous mass is gas.

Keywords: downward continuation, density contrast, residual gravity anomaly, depth, density log

1 Introduction

The process by which potential field data from one datum surface (in this case, residual gravity anomaly) are mathematically projected downward to level surfaces below the original surface is known as downward continuation. This is a direct approach to the quantitative interpretation of residual Bouguer anomalies, when specific models are not used to represent the geological structures (Grant and West, 1987, Keary and Brooks 2002). It is used to increase the resolution of weak anomalies by projecting the field to a level closer to the source of the anomaly (Telford et al, 1990). The process is adopted in this research is based upon the concept of equivalent stratum. Equivalent stratum means the process in which gravitational field whose normal component is given on a horizontal plane can be related to a surface distribution of density on that plane (Grant and West, 1987). This is particularly relevant when an interface between two materials having different formation densities has been identified at some known or estimated depth by means other than gravity surveying. This process is always difficult to interpret because of inherent uncertainties in the location and size of the structure represented by the Bouguer gravity at the datum plane. This

ambiguity is caused by the anomalous masses lying between surfaces and the desired depth of projection, which causes fluctuation in the gravity values at intermediate levels (Grant and West, 1987, Dobrin and Savit, 1988). In downward continuation, an important aspect of the underlying theory is that when the field is continued too close to the depth of the anomalous mass, oscillations set in due to the instability of the field at that point. It becomes stabilized within the horizon of the anomalous mass and oscillation and divergence re-appears when the projected field is beyond the horizon of the anomalous mass. The object of the interpretation is then to determine the relief on this surface which is compatible with the observed variations in Δg . The difficulties posed by such a contingency are resolved with the aid of additional subsurface data. In this research, density log was utilized in the downward continuation process.

In the use of density log, the determination of the weighting density function is crucial. In this case, the attenuation constant is required to be made as small as practicable such that the weighting density distribution changes in sign within a distance which is not more than the average spacing between the gravity stations. This helps in the presentation of a plausible subsurface structure of the basin from the projected fields. The minimization of the attenuation constant is accomplished in this paper by establishing a mathematical model which relates the attenuation constant as a function of the residual gravity anomaly wave numbers, the gravity station spacing and the depth of projection.

2 Model Formulation

2.1 The Theory of Equivalent Stratum

Consider a material to be distributed with a surface density $\rho(x, y)g/cm^2$ of the horizontal plane $z = 0$. To calculate the gravitational field of this coating at a point Q in $z = 0$, a set of circular cylindrical coordinates (r, ϕ, z) is chosen, whose

axis is vertical and whose origin is placed at Q as shown in Figure 1. At a point P on the axis, gravitational potential will be (Grant and West, 1987):

$$U_p = -G \int_0^\infty \int_0^{2\pi} \frac{\rho(r, \phi)}{\sqrt{r^2 + z^2}} r d\phi dr \quad (1)$$

Where ρ is the surface density, U_p = gravitational potential at P, r = radius, z = horizontal plane.

Gravitational field at P is given as:

$$P = -\nabla U_p \quad (2)$$

Since the potential U is due to masses that are locally distributed on $z = 0$, the gravity effect at P is written as

$$\Delta g_p = -\frac{\partial U_p}{\partial z} = G|z| \int_0^\infty \int_0^{2\pi} \frac{\rho(r, \phi)}{(r^2 + z^2)^{3/2}} r d\phi dr \quad z < 0 \quad (3)$$

The negative sign being used because Δg is to be measured in the direction of g . It is required to evaluate the integral in the limit as $z \rightarrow 0$ by utilizing a small circle at Q of radius ε which is finite. The radius ε is chosen such that throughout the circle $\rho(x, y)$ does not change appreciable from its value at Q . This gives (Grant and West, 1987):

$$\Delta g_p = G\rho(Q)|z| \int_0^\infty \int_0^{2\pi} \frac{rd\phi dr}{(r^2 + z^2)^{3/2}} = 2\pi G\rho(Q) \left(1 - \frac{|z|}{\sqrt{\varepsilon^2 + z^2}}\right) \quad (4)$$

This finally gives:

$$\Delta g(Q) = 2\pi G\rho(Q) \quad (5)$$

But the position of Q in $z = 0$ is arbitrary, so that we may write

$$\Delta g(x, y) = 2\pi G\rho(x, y) \quad (6)$$

Suppose that the gravity effect $\Delta g(x, y)$ on $z = 0$ is produced by an unknown distribution of matter below this plane. Then whatever the array of masses may actually be, its effect at any point in $z \leq 0$ would be exactly the same if it were replaced by the surface distribution on $z = 0$ given by equation 6. This density

coating is therefore called the equivalent stratum for the unknown distribution of matter in $z > 0$.

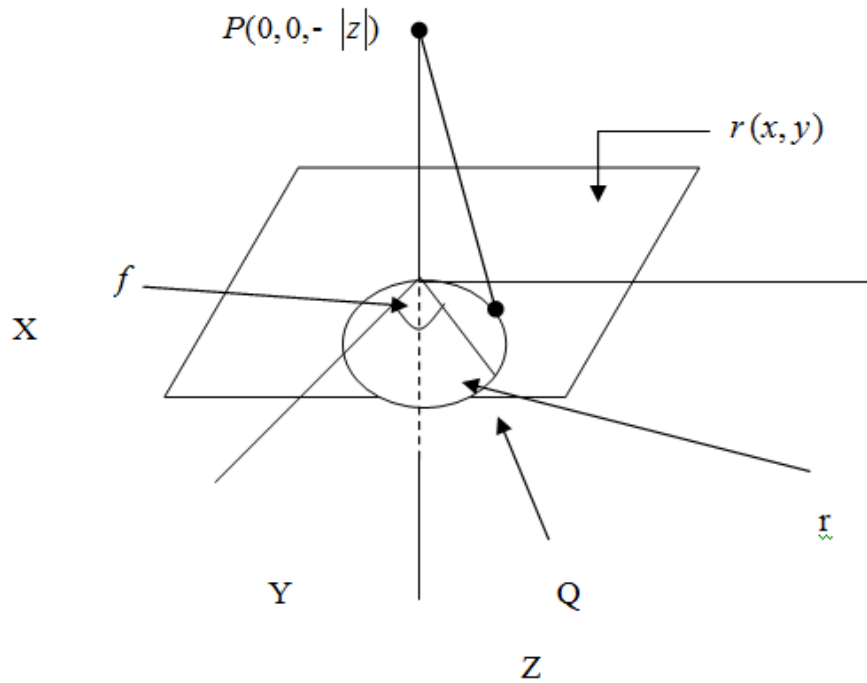


Figure 1: The “equivalent Stratum” (Source: Grant and West 1987)

2.2 Downward Continuation Model Formulation Using Density log

The method adopted in this research, is the calculation of equivalent stratum at the given depth and then replace it with the topographic surface $h(x, y)$, which is given by

$$\sigma(x, y) = \Delta\rho h(x, y) \quad (7)$$

Where $\Delta\rho$ is the difference in the formation densities between the two media.

This formula can be explained by referring to Figure 2.

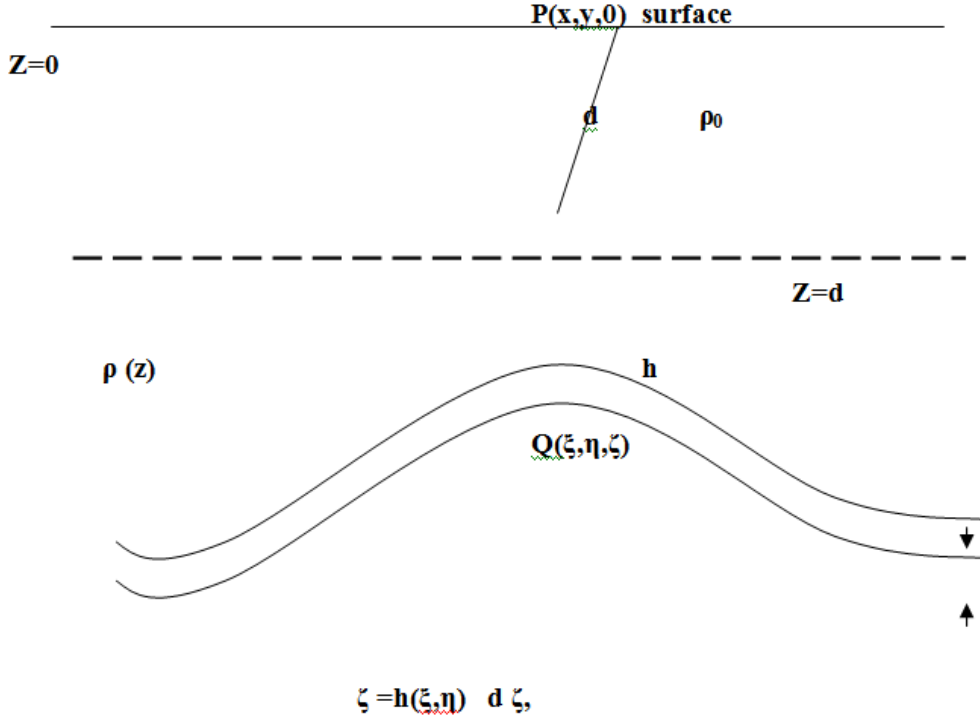


Figure 2: Shows the use of downward continuation when a continuous density log is available (Source: Grant and West 1987)

Suppose that $h(x, y)$ is the vertical departure of the interface at any point from its mean depth d , then the vertical effect at $P(x, y)$ due to the undulation in the interface will be (Grant and West 1987):

$$\Delta\rho(z) = \rho(z) - \rho_0 \quad (8)$$

we consider the change in gravity at the surface due to relief h in the thin stratum at depth $\zeta \geq d$ whose thickness is $d\zeta$.

$$\Delta g(x, y) = -G \int_d^{d+h(\xi, \eta)} \Delta\rho(\zeta) \left(1 + \zeta \frac{\partial}{\partial \zeta} \right) \int_{\xi=1}^2 \int_{\eta=1}^2 \frac{h(\xi, \eta) d\xi d\eta}{((x-\xi)^2 + (y-\eta)^2 + \zeta^2)^{3/2}} d\zeta, \quad (9)$$

taking the Fourier transform on both sides with respect to x and y

$$F(p, q) = (2\pi)^{-1} GH(p, q)X(p, q), \quad (10)$$

where H is the Fourier transform of h ,

$$\begin{aligned} X(p, q) &= -\int_d^{d+h(\xi, \eta)} \Delta\rho(\zeta) \left(1 + \zeta \frac{\partial}{\partial \zeta}\right) \frac{\exp(-\sqrt{p^2 + q^2} \zeta)}{\zeta} d\zeta \\ &= \sqrt{p^2 + q^2} \int_d^{d+h(\xi, \eta)} \Delta\rho(\zeta) \exp(-\sqrt{p^2 + q^2} \zeta) d\zeta, \end{aligned} \quad (11)$$

where

$d\zeta$ = thickness,

$\rho(\zeta)$ = density values obtained from the borehole measurement,

ρ_0 = formation density of the chosen depth.

To find h , we transpose equation 9 and perform the Fourier inversion.

Further treatment of Fourier analysis can be found in (Kopal 1960), (Grant and West, 1987). The expression for the downward continuation of gravity effect at depth Z_n is given by:

$$\Delta g(x, y)_{Z_n} = \frac{1}{2\pi} X(\gamma) \Delta g_0(x, y), \quad (12)$$

where $\Delta g(x, y)_{Z_n}$ is the residual gravity anomaly value at depth Z_n ,

$\Delta g_0 \Delta g(x, y)_{Z_n}$ is the residual gravity anomaly value at the surface,

$X(\gamma)$ = weighting density function.

$$X(\gamma) = \Delta\rho_n e^{\gamma z_n} \quad (13)$$

$$\Delta\rho_n = \rho_{n+1} - \rho_0, \quad (14)$$

where

$\Delta\rho_n$ is the density contrast,

ρ_0 = formation density of the chosen depth,

ρ_{n+1} = formation density of the preceding layer,

γ = attenuation constant

$$\gamma = \frac{s^2}{d^2} \sqrt{p^2 + q^2} \quad (15)$$

where $p = \frac{\pi}{x_m}$, $q = \frac{\pi}{y_m}$

p, q = wave numbers, s = distance between stations, d = initial chosen depth from the log x_m , and y_m = measured distances between points at which Δg takes the value $\frac{1}{2} \Delta g_{\max}$ in these two directions with respect to the well location.

Equation 13 shows that as we move towards the anomaly source, all wave numbers are attenuated by $e^{-\gamma z_n}$ and that the highest wave numbers (shortest wavelengths) are attenuated most rapidly. The density contrast defines the basement control over the anomalous mass.

$$Z_n = d + h, \quad (16)$$

where h , the constant depth interval = 155m, d is the initial chosen formation depth = 1710m.

3 Methodology

3.1 Data Acquisition

The gravity data and density log observation used in this research were obtained from Shell Nigeria Exploration and Production (SNEPCO). They gravity data contain a total of 1813 gravity stations with a station interval of 500m. The field work was carried out by Compagnie Generale de Geophysique (CGG) and the project area is OPL 803/806/809 respectively. The density log observation was obtained from Kolmani River of the project area which lies in the closure C of the residual gravity anomaly.

3.2 The Downward Continuation Computation

The downward continuation concept for vertical gravity variation was carried out using equation (12).

In this research, the $\rho(z)$ was replaced with a number of constant formation densities by dividing up the density log into shorter sections at constant interval of 155m. The initial formation depth d is taken as 1710m and the formation density at that depth is given as 2.1g/cm^3 . The other depths and their formation densities are as shown below in Table 1.

Table 1: Well log Formation Depth and Density Values

S/N	Depth(m)	Density(g/cm^3)	Density contrast (g/cm^3)
1	1860	2.00	-0.10
2	2015	2.30	0.20
3	2170	2.40	0.30
4	2325	2.86	0.76
5	2480	2.40	0.30

4 Results and Analysis

4.1 Results

The map of the residual gravity anomaly of the basin is shown in Figure 3. The results obtained for the downward continuation at 1860m, 2015m, 2170m and 2325m and 2480m are shown in Figures 4 to 8 respectively.

4.2 Analysis of Results

4.2.1 Map of Depth 1860m

At the depth of 1860m, the residual gravity anomaly values were all positives. This does not correlate with the geology of the basin. This is as a result of the negative density contrast between the initial formation depth of 1710m and the projection depth. The residual gravity anomaly at this depth was at sharp variance with that projected from the surface. The shape of closure at C on the projected field was not well defined. The minimum residual value is 5mGal in the south-east, while the maximum value is 60mGal in the north-east of the project. The residual gravity anomaly value at closure C is 5mGal as shown in Figure 4.

4.2.2 Map of Depth 2015m

At the depth of 2015m, the residual gravity values are negative which correlates with the geology of the basin. All the closures reflect the same structural feature as that projected from the surface. However, the closure at C along the composite profile (94V071/95D071/94V037) was better established than that obtained at depth 2015m. This is an indication of the expected oscillation of the residual values suggesting that the depth is closer to the anomalous mass. The maximum residual anomaly value is -10mGal in the south-west, while the minimum value is -140mGal in the north-east of the project. The residual value within the closure at C is -40mGal as shown in Figure 5.

4.2.3 Map of Depth 2170m

At the depth of 2170m, the residual gravity anomaly values are negative. This correlates with the geology of the area. Also, the closure at C location along the composite profile reflects the structural feature as that obtained at depth 2015m. The maximum residual anomaly value is -10mGal in the south-west,

while the minimum value is -260mGal in the north-east of the project. The residual value within the trap C area is -10mGal as shown in Figure 6.

4.2.4 Map of Depth 2325m

At the depth of 2325m, the residual gravity anomaly values are negative. This correlates with the geology of the area. Also, the trap C location along the composite profile (as shown in Figure 7) does not reflect the structural feature as that obtained at depth 2015 and 2170m. The maximum residual anomaly value is 50mGal in the south-west, while the minimum value is -700mGal. The residual value within the closure at C area is -200mGal. The residual anomaly values obtained at this depth is exponentially amplified. It shows a divergence from that obtained at depths 2015m and 2170m respectively.

4.2.5 Map of Depth 2480m

At the depth of 2480m, the residual gravity anomaly values are negative. This correlates with the geology of the area. Also, the trap C location along the composite profile (as shown in Figure 8) reflects the structural feature as that obtained at depth 2015 and 2170m. The maximum residual anomaly value is -100mGal in the south-west, while the minimum value is -400mGal. The residual value within the closure at C area is -100mGal. The residual anomaly values obtained at this depth shows a similar value with that obtained at 2015m and 2170m. It shows that the values are beginning to oscillate with respect to that obtained at the previous depths.

4.2.6 Summary of Findings

1. The new formulated weighted density function provided a good estimate of the maximum gravity effect that can be expected from a topographic feature of a given size which lies at a given depth.
2. Fluctuation in the residual gravity anomaly values between negative and positive at intermediate levels showed that the attenuation was minimized in the new formulation.
3. The new weighting density function is robust and is applicable to any basin.
4. The residual gravity anomaly values were amplified with increasing depth showing that the residual features are controlled by the basement.
5. The depth of 2015m and 2170m in which the residual structure was stable defines the lower and upper limits of the anomalous mass.
6. The density contrast between the depth of 1860 and 2325m is 0.86g/cc suggesting that the anomalous mass is gas.

5 Conclusion

The weighting density function obtained from the well data provided the sampling density required in the determination of the vertical and lateral lithologic variations of the basin. The residual gravity anomaly provided the areal sampling coverage but cannot be used alone in defining the multiple interfaces that contribute in its observation at the surface due to the gravitational inverse problem. When the two datasets are integrated, they provide a better depth, lithology and prospect definitions within a basin.

Acknowledgement. We thank Shell Nigeria Exploration and Production Company (SNEPCO) for the release of the data used in this research.

References

- [1] C.O. Ajayi and D.E. Ajakaiye, Structures Deduced From Gravity Data In The Middle Benue, Nigeria, *Journal of African Earth Sciences*, **56**, (1986), 80-89.
- [2] V. Barbosa, B. Joao and W. Medeiros, Gravity Inversion of Basement Relief Using Approximate Equality Constraints on Depth, *Geophysics*, **6**, (1997), 1745-1757.
- [3] E.L. Bigelow and R.F. Hertz, *Fundamental Of Diplog Analysis*, Atlas Wireline Seivices, Western Atlas International Inc. Texas, 1993.
- [4] R.J. Blakely, *Potential Theory in Gravity and Magnetics Application*, Cambridge University Press, Cambridge, 1996.
- [5] D.K. Butler, Micro Gravimetric and Gravity Gradient Technique for Detection of Subsurface Cavities, *Journal of Geophysics*, **49**(7), (1984), 084-1096.
- [6] U. Casten and C. Gram, Recent Development In Underground Gravity Surveys, *Geophysical Prospecting Journal*, **37**(1), (1989), 73-90.
- [7] Y. Chai and W.J. Hinze, Gravity Inversion Of An Interface Above Which The Density Contrast Varies Exponentially With Depth, *Journal of Geophysics*, **53**(2), (1988), 837-845.
- [8] D. Chenot and N. Debeglia, Three Dimensional Gravity and Magnetic Constrained Depth Inversion With Lateral And Vertical Variation Contrast, *Journal of Geophysics*, **55**(15), (1990), 327-335.
- [9] D. Bhaskara Rao, Modeling of Sedimentary Basins from Gravity Anomalies with Variable Density Contrast, *Geophysical Journal of the Royal Astronomical Society*, **84**(1), (1985), 207-212.
- [10] R.J. Blakely, *Potential Theory in Gravity and Magnetics Application*, Cambridge University Press, Cambridge, 1996.
- [11] V. Chakravarthi and N. Sundararajan, Ridge Regression Algorithm for Gravity inversion of fault structures with variable Density, *Geophysics*, **69**, (2004), 1394-1404.

- [12] V. Chakravarthi and N. Sundararajan, Automatic 3-D gravity modeling of sedimentary basins with density contrast varying parabolically with depth, *Comput. Geosci*, **30**, (2004), 601-607.
- [13] V. Chakravarthi and N. Sundararajan, *3D gravity inversion of basement relief –A depth-dependent density approach*, Society of Exploration Geophysics Digital Library, 2007.
- [14] V.E. Darwin and M.S. Julian, *Well Logging for Earth Scientists*, McGraw-Hill Companies Inc. USA, 2007.
- [15] J. David and K. Pile, *Well Logging in Non-Technical Language*, 2nd edition, Penn Well Publishing Company, Tulsa, Oklahoma, 2002.
- [16] J.T. Dewan, *Essentials of Model Open-Hole Log Interpretation*, Pennwell Publishing Company, Tulsa, Oklahoma, p. 301, 1995.
- [17] M.B. Dobrin and C.H. Savit, *Introduction to Geophysical Prospecting*, 4th edition, Singapore, McGrawHill Book Co, p.867, 1988.
- [18] Z. Fajkiewicz, Origin of The Anomalies Of Gravity And Its Vertical Gradient Over Cavities In Brittle Rock, *Journal of Geophysical Prospecting*, **34**(8), (1986), 1233-1254.
- [19] H. Granser, Three Dimensional Interpretation of Gravity Data from Sedimentary Basin using An Exponential Density-Depth Function, 48th EAEG Conference, Ostend, (1986).
- [20] F.S. Grant and G.F. West, *Interpretation Theory in Applied Geophysics*, McGrawhill Book Company, Toronto, p. 584, 1987.
- [21] F. Gupsi, Non-Iterative Non-Linear Gravity Inversion, *Journal of Geophysics*, **58**(7), (1983), 935-940.
- [22] H. James, *Introduction to Geophysical Formation Evaluation*, CRC Press, LLC, Florida, USA, 2000.
- [23] F. John, *Shared Earth Modeling- Methodologies for Integrated Reservoir Simulations*, Elsevier Science, USA, 2002.
- [24] Z. Kopal, *Numerical Analysis*, Chapman and Hall, London, 1960.

- [25] J. Maxant, Variation of Density with Rock Type, Depth and Formation in Western Canada Basin from Density Logs, *Journal of Geophysics*, **45**(6), (1980), 1061-1076.
- [26] D.W. Oldenburg, The Inversion and Interpretation of Gravity Anomalies, *Geophysics*, **39**, (1974), 526-536.
- [27] I.L. Nettleton, *Gravity and Magnetism In Oil Prospecting*, New York, McGraw Hill, 1976.
- [28] S. Obert, *Fundamentals of Well-log Interpretation*, Elsevier Science Publishers, Netherland, 2001.
- [29] R.L. Parker, The Rapid Calculation of Potential Anomalies, *Geophysics, J. Roy. Astr. Soc.*, **31**, (1973), 447-455.
- [30] M. Pilkington and D. Crossley, Determination of Crustal Interface Topography from Potential Fields, *Geophysics*, **51**, (1986), 1277-1284.
- [31] D.B. Rao, Gravity Anomalies of two Dimensional Bodies with Density Contrast Varying with Depth, *Journal of Geophysics*, **44**(5), (1979), 177-182.
- [32] D.B. Rao, Analysis of Gravity Anomalies of Sedimentary Basin by Trapezoidal Model with Quadratic Density Function, *Journal of Geophysics*, **55**(2), (1990), 226-231.
- [33] M.H. Rider, *The Geological Interpretation of Well Logs*. Rider-French Consulting Ltd, Sutherland, Scotland, p. 280, 2006.
- [34] N. Ronald, *Geologic Analysis of Naturally Fractured Reservoir*, 2nd edition, Butterworth-Heineman, Wildwood Avenue, Woburn, USA, 2001.
- [35] Schlumberger *Log Interpretation Principles/Applications*, Schlumberger Educational Series, 1993.
- [36] M. Stefan, *Geological Well Logs: Their Use in Reservoir Modeling*, Springer-Verlag, Berlin, Germany, 2001.
- [37] J.P. Sylvian, *Geologic Well Log Analysis*, Gulf Publishing Company, USA, p. 369, 1977.
- [38] J.P. Sylvian, *Handbook of Well Log Analysis for Oil and Gas Formations*,

Prentice Hall Inc, Eaglewood Cliff, 1979.

- [39] W.M. Telford, C.P. Geldart, R.T. Sheriff, and D.A. Keys, *Applied Geophysics*, Cambridge University Press, p. 852, 1990.
- [40] D. Toby, *Well Logging and Formation Evaluations*, Elsevier Inc, USA, 2005.
- [41] L. Vadim, Concept of Effective Density: Key to Gravity Depth Determination for Sedimentary Basins, *Geophysics*, **54**, (1989), 1474.

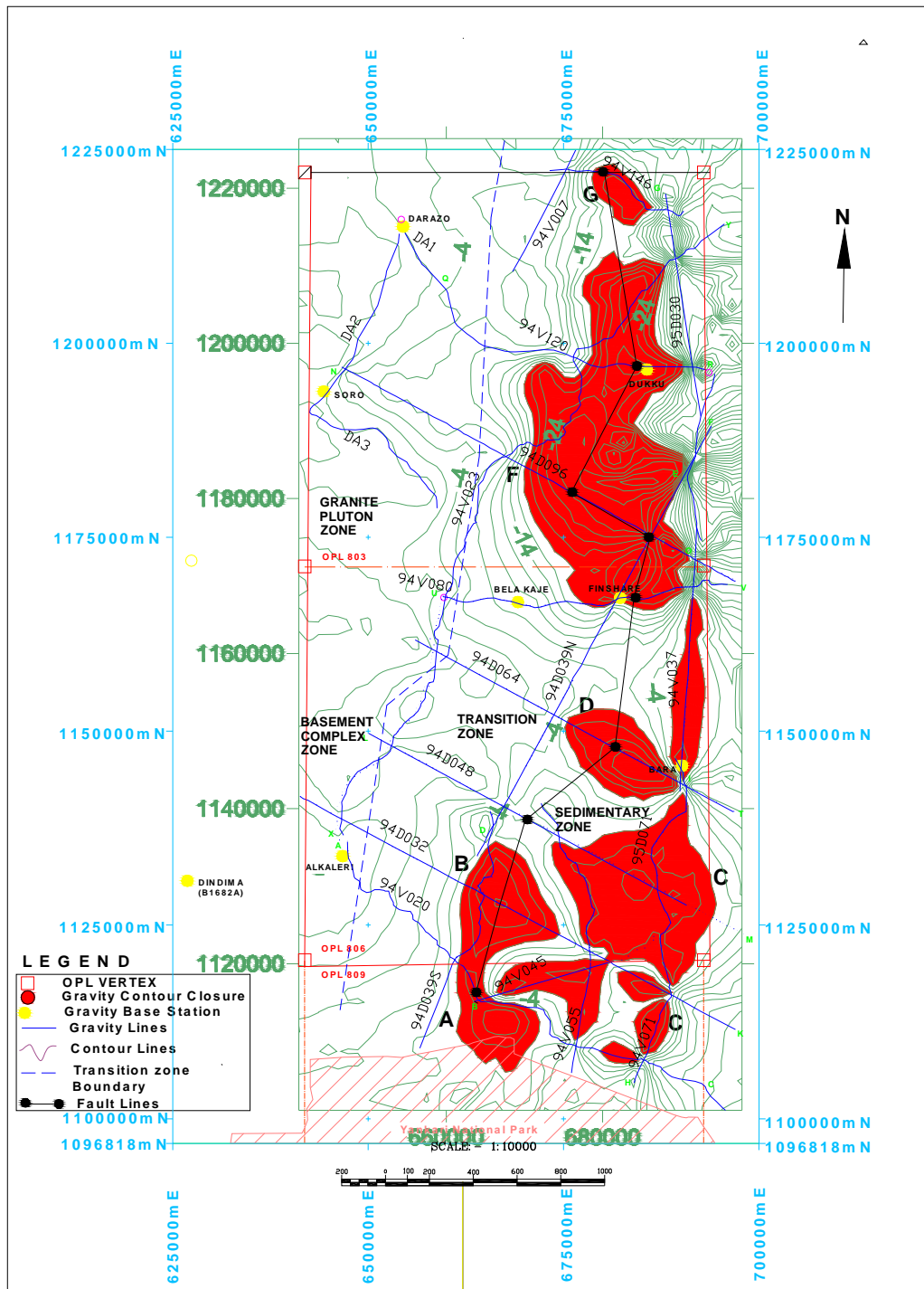


Figure 3: Residual Anomaly Map of the Basin (C.I =1mGal)

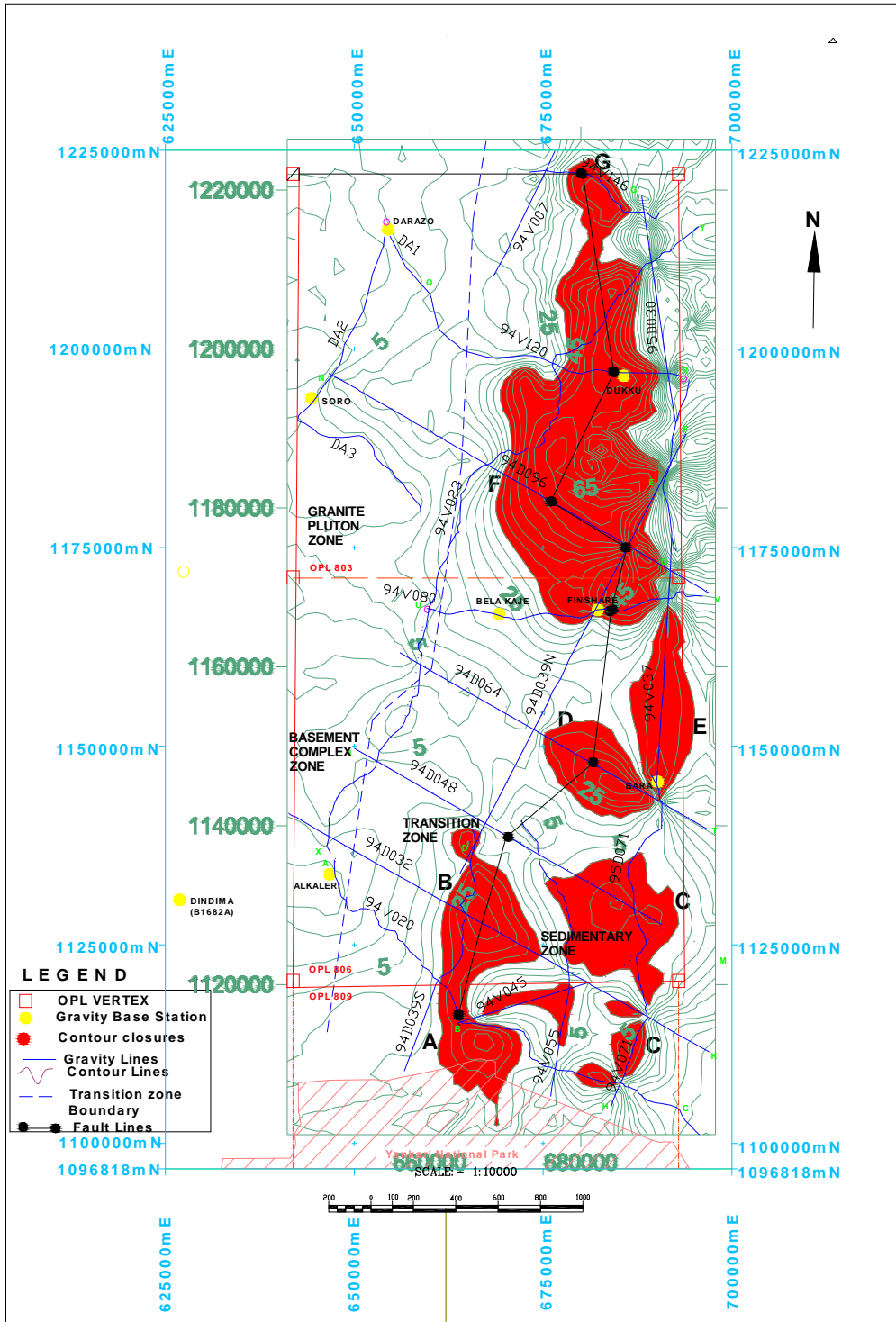


Figure 4: Downward Continuation Map for Depth 1860m (C.I.: 5mGal)

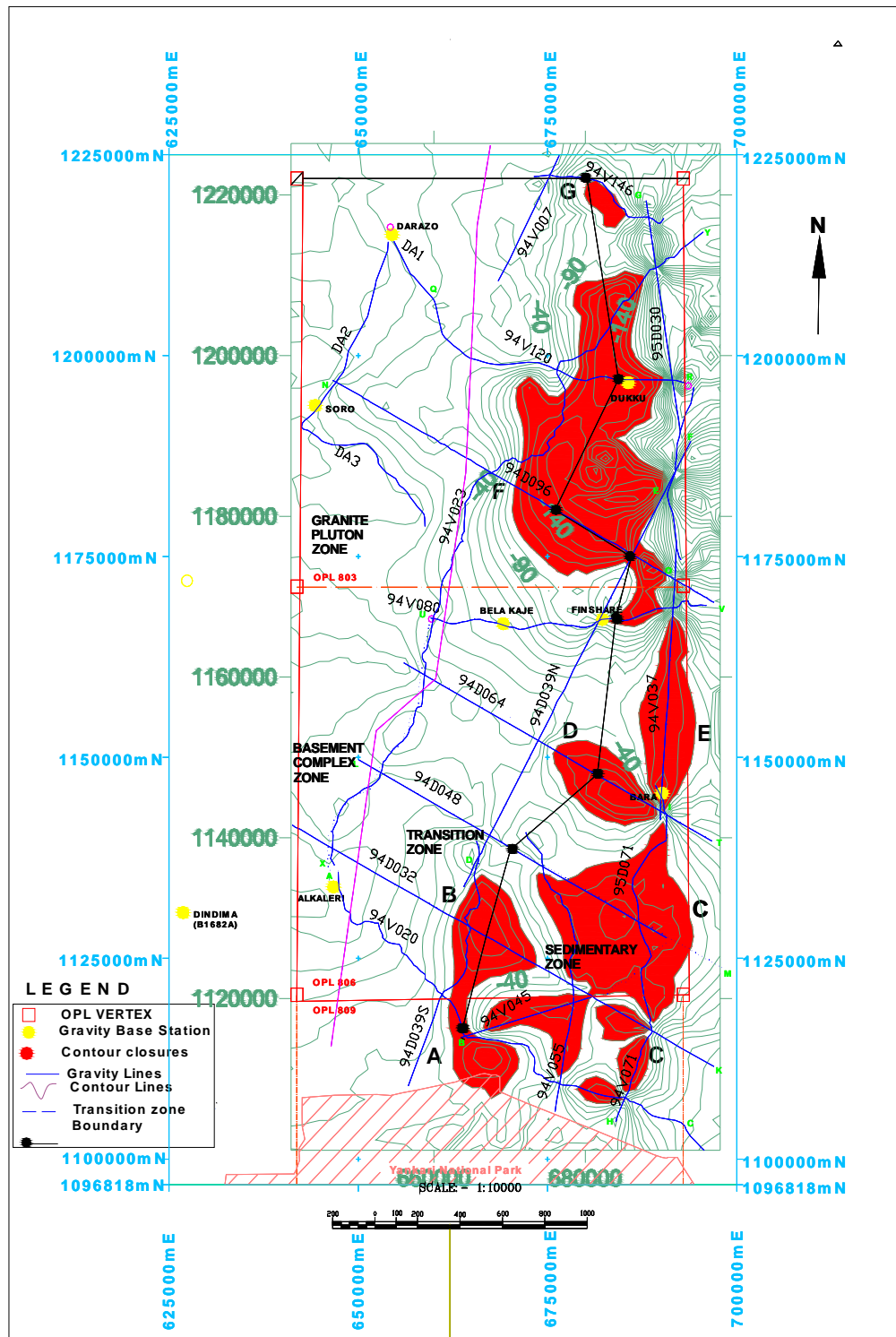


Figure 5: Downward Continuation Map for Depth 2015m (C.I : 3mGal)

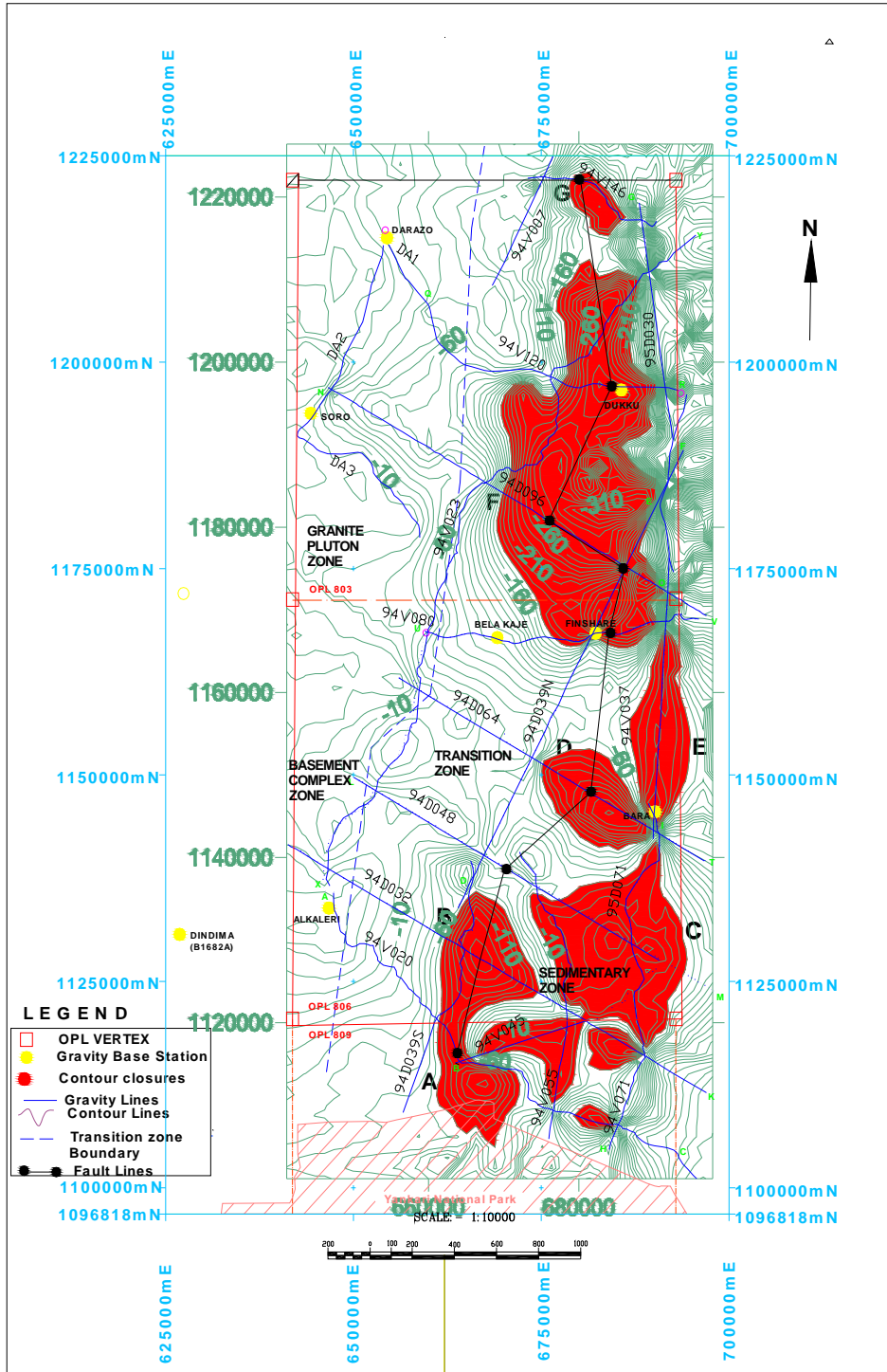


Figure 6: Downward Continuation Map for Depth 2170m (C.I : 10mGal)

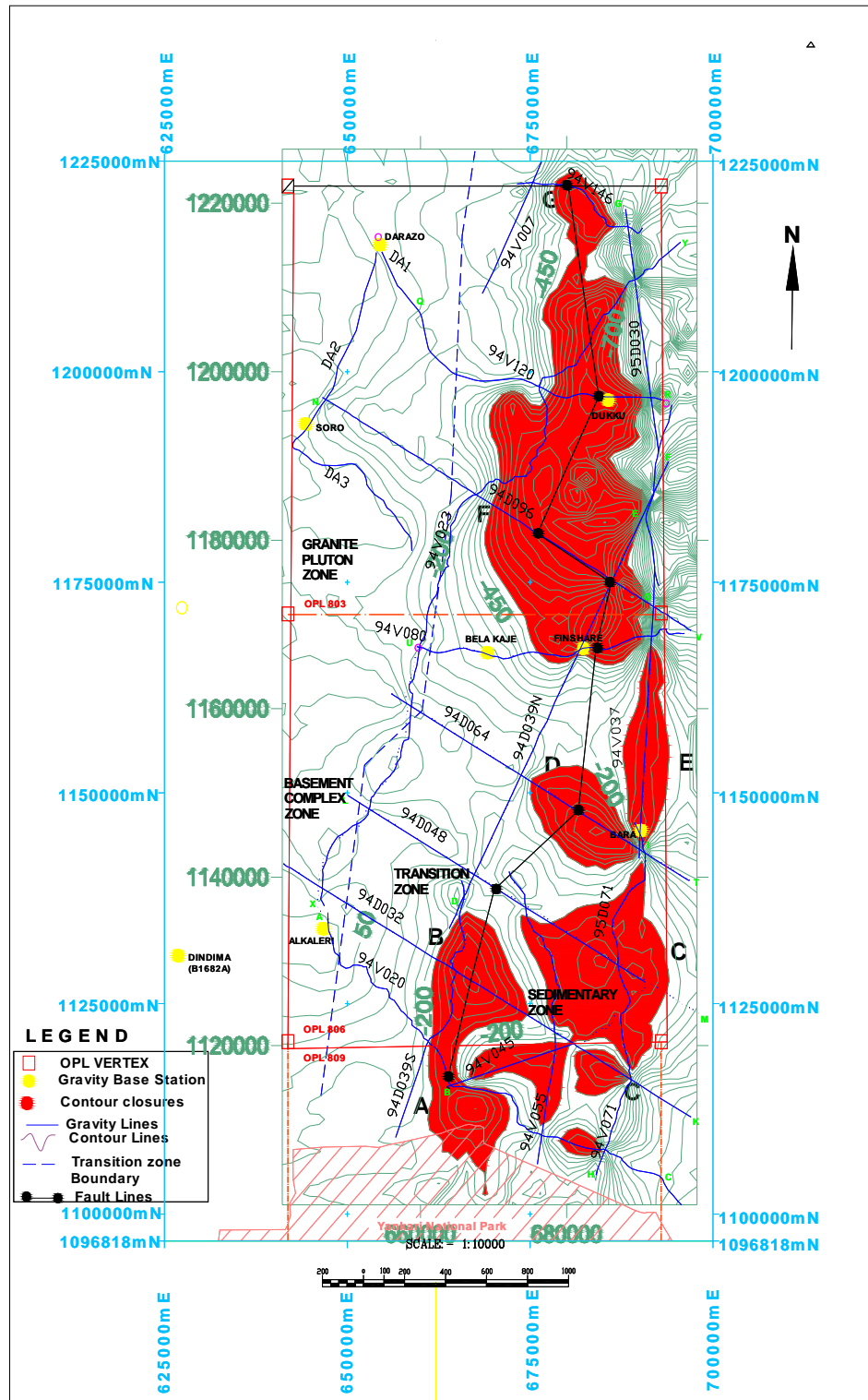


Figure 7: Downward Continuation Map for Depth 2325m (C.I: 50mGal)

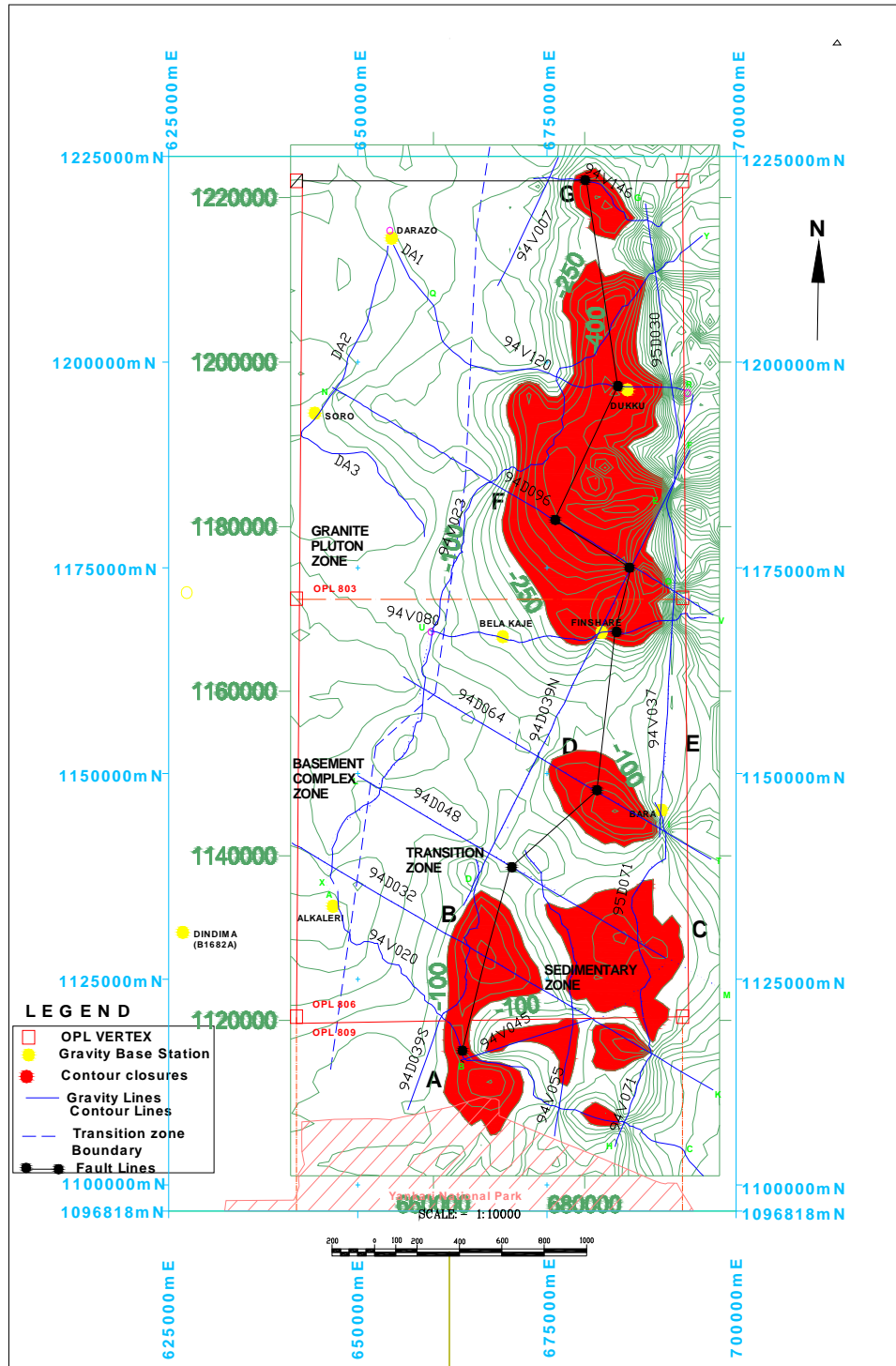


Figure 8: Downward Continuation Map for Depth 2480m (C.I: 30mGal)